

1em 0pt

LME-MPM applied to quasi-brittle fracture.

Miguel Molinos^a, and Pedro Navas^{a1}

^a *ETSI Caminos, Canales y Puertos, Universidad Politécnica de Madrid.*
c. Prof. Aranguren 3, 28040 Madrid, Spain

Abstract

The objective of this work is to introduce an alternative technique to address the fracture process of brittle and quasi-brittle materials under the material point method (MPM) framework. With this purpose the eigensoftening algorithm, developed originally for the optimal transportation mesh-free (OTM) approximation scheme, is extended to the MPM with the aim of present a suitable alternative to the existing fracture algorithms developed for the MPM. The good fitting in the predictions made by the eigensoftening algorithm against both analytical and experimental results proofs the well performance of the method under challenging loads.

Keywords: Quasi brittle fracture, Local-*max-ent* approximation, Material Point Method, Solid Dynamics

1. Introduction

The simulation of fracture propagation in a more accurate and effective way can be considered as one of the original drivers for developing novel spatial discretization methods such as meshfree methods like the material
5 point method (MPM). Presence of cracks are a violation of the continuity requirement of the finite element method (FEM).

By contrast, MPM does not suffer from the above difficulty since the continuity requirement is less restrictive. Regarding fracture, it can be described in two ways. One is to remove the restriction of the single-valued
10 velocity field close to the crack by using two or more sets of nodes [1]. This method is based in to assign different labels to distinguish if the material points and nodes are in the same side of the crack or not. Under this approach the crack surface is described with line segments in 2D and triangle patches in 3D cases. This method was named as “CRACKs with Material

¹Corresponding author: p.navas@upm.es

15 Points (CRAMP)” [2]. In this method, the criteria for crack propagation is based on such parameters as energy release rate analyzed by Tan & Nairn (2002)[3], and the stress intensity factor or the J-integral discussed by Guo & Nairn (2004)[4].

and the other is to use failed material points to describe the crack evolu-
20 tion.

The erosion of the material point means that each material point can be either intact or be completely failed or eroded and has no load bearing capacity, Even though the method has been successfully applied to dynamic fragmentation of metals, quantitative validations, such as stress or strain
25 levels near or at the crack set compared to experimental measures are still lacking. Having in mind that the eigenerosion approach was intended for perfectly brittle fracture, an eigensoftening concept is developed for quasi-brittle materials

2. The meshfree methodology

30 The aim of this section is to provide an overview of the special techniques employed to face the fracture problem under the MPM framework. In consequence it is structured as follows: first in 2.1 we summarize the explicit-predictor algorithm for the MPM, next the local *max-ent* approximants are introduced in 2.2 as an accurate alternative technique to interpolate data
35 between particles and nodes, and finally the fracture algorithms based in the eigendeformations are presented in 2.3.

2.1. The Material Point Method

The MPM [5] is a meshfree Lagrangian-Eulerian method where particles carries on all the physical information and a set of background nodes is employed to compute the equilibrium equation. Since the MPM possesses the advantages of both Lagrangian and Eulerian descriptions, no element distortion exists in the MPM, therefore it is an appropriate and efficient method in solving problems involving extremely large deformation and moving discontinuities such fracture evolution. For the spatial discretization, two sets of points are introduced in the MPM. First, the nodes. These points are considered fixed in the space and are in charge of computing all the kinematic fields such forces f_I , accelerations a_I and velocities v_I . And second the material points or particles. They are in charge of the discretization of the continuum, and store the local state $(\sigma_p, \varepsilon_p)$. Without losing generality, the MPM algorithm can be described with three main steps: (i) a variational recovery process, where particle data is projected to the grid nodes, (ii) an Eulerian

step, where balance of momentum equation is expressed as a nodal equilibrium equation thorough a FEM-like procedure, and finally (iii) a Lagrangian advection of the particles. In the present research we will adopt a explicit predictor-corrector time integration scheme. The purpose of this choice is motivated due its proved robustness and stability in numerical calculations. In the first stage (i), the nodal velocity predictor is computed following (1),

$$\vec{v}_I^{k+1} = \frac{N_{Ip}^k m_p (\vec{v}_p^k + (1 - \gamma) \Delta t \vec{a}_p^k)}{m_I} \quad (1)$$

This way of computing the nodal predictor is both numerically stable and minimize the computational effort. Once nodal velocity are obtained, the essential boundary conditions are imposed. And in the following, a Eulerian phase (ii) is computed in the set of nodes in a FEM-like way, where nodal forces \vec{f}_I^{k+1} are computed thorough the equilibrium equation. Next the nodal velocities are corrected in a *corrector* stage,

$$\vec{v}_I^{k+1} = \vec{v}_I^{pred} + \gamma \Delta t \frac{\vec{f}_I^{k+1}}{\mathbf{m}_I^{k+1}} \quad (2)$$

Finally updated the particles are advected in the Lagrangian stage (iii) using nodal values as,

$$\vec{a}_p^{k+1} = \frac{N_{Ip}^k \vec{f}_I^k}{\mathbf{m}_I^k} \quad (3)$$

$$\vec{v}_p^{k+1} = \vec{v}_p^n + \Delta t \frac{N_{Ip}^k \vec{f}_I^k}{\mathbf{m}_I^k} \quad (4)$$

$$\vec{x}_p^{k+1} = \vec{x}_p^n + \Delta t N_{Ip}^k \vec{v}_I^k + \frac{1}{2} \Delta t^2 \frac{N_{Ip}^k \vec{f}_I^k}{\mathbf{m}_I^k} \quad (5)$$

The complete pseudo-algorithm it is summarized in Appendix A.

2.2. Spatial discretization : Local-max-ent approximants

Local maximum-entropy (or local *max-ent*) approximation scheme was introduced by Arroyo & Ortiz (2006)[6] as a bridge between finite elements and meshfree methods. The key idea of the shape functions is to interpret the nodal of a shape function N_I as a probability. This allow us to introduce two important limits: the principle of maximum-entropy (*max-ent*) statistical inference stated by [7], and the Delaunay triangulation which ensures the

minimal width of the shape function. To reach to a compromise between two competing objectives, a Pareto set is defined as,

$$\begin{aligned}
 &(\text{LME})_\beta \text{ For fixed } \vec{x} \text{ minimise } f_\beta(\vec{x}_p, N_I) = \beta U(\vec{x}_p, N_I) - H(N_I) \\
 &\text{subject to } \begin{cases} N_I \geq 0, \text{ I}=1, \dots, n \\ \sum_{I=1}^{N_n} N_I = 1 \\ \sum_{I=1}^{N_n} N_I \vec{x}_I = \vec{x} \end{cases}
 \end{aligned}$$

where $H(N_I)$ is the entropy of the system of nodes following the definition given by Shannon (1948) [8], and $U(\vec{x}_p, N_I) = \sum_I N_I |\vec{x}_p - \vec{x}_I|^2$ a magnitude of the shape function width. The regularization o *thermalization* parameter between the two criterion β has Pareto optimal values in the range $(0, \infty)$. The unique solution of the local max-ent problem $(\text{LME})_\beta$ is:

$$N_I^*(\vec{x}) = \frac{\exp \left[-\beta |\vec{x} - \vec{x}_I|^2 + \vec{\lambda}^* \cdot (\vec{x} - \vec{x}_I) \right]}{Z(\vec{x}, \vec{\lambda}^*(\vec{x}))} \quad (6)$$

where $Z(\vec{x}, \vec{\lambda}^*(\vec{x}))$ is the *partition function* defined as,

$$Z(\vec{x}, \vec{\lambda}) = \sum_{I=1}^{N_n} \exp \left[-\beta |\vec{x} - \vec{x}_I|^2 + \vec{\lambda} \cdot (\vec{x} - \vec{x}_I) \right] \quad (7)$$

40 and evaluated in the unique minimiser $\vec{\lambda}^*(\vec{x})$ for the function $\log Z(\vec{x}, \vec{\lambda})$. The traditional way to obtain such a minimiser is using (8) to calculate small increments of $\partial \vec{\lambda}$ in a Newton-Raphson approach. Where \mathbf{J} is the Hessian matrix, defined by:

$$\mathbf{J}(\vec{x}, \vec{\lambda}, \beta) \equiv \frac{\partial \vec{r}}{\partial \vec{\lambda}} \quad (8)$$

$$\vec{r}(\vec{x}, \vec{\lambda}, \beta) \equiv \frac{\partial \log Z(\vec{x}, \vec{\lambda})}{\partial \vec{\lambda}} = \sum_I^{N_n} p_I(\vec{x}, \vec{\lambda}, \beta) (\vec{x} - \vec{x}_I) \quad (9)$$

In order to obtain the first derivatives of the shape function ∇N_I^* , can be computed as,

$$\nabla N_I^* = N_I^* \left(\nabla f_I^* - \sum_J^{N_n} N_J^* \nabla f_J^* \right) \quad (10)$$

where

$$f_I^*(\vec{x}, \vec{\lambda}, \beta) = -\beta |\vec{x} - \vec{x}_I|^2 + \vec{\lambda}^* (\vec{x} - \vec{x}_I) \quad (11)$$

Employing the chain rule over (10), rearranging and considering β as a constant, Arroyo and Ortiz [6] obtained the following expression for the gradient of the shape function.

$$\nabla N_I^* = -N_I^* (\mathbf{J}^*)^{-1} (\vec{x} - \vec{x}_I) \quad (12)$$

The regularization parameter β of LME shape functions may be controlled by adjusting a dimensionless parameter, $\gamma = \beta h^2$ [6], where h is defined as a measure of the nodal spacing. Since N_I is defined in the entire domain, in practice, the shape function decay $\exp(-\beta r)$ is truncated by a given tolerance, 10^{-6} , for example, would ensure a reasonable range of neighbours, see [6] for details. This tolerance defines the limit values of the influence radius and is used thereafter to find the neighbour nodes of a given integration point.

2.3. Fracture modelling approach

Within the context of MPM formulation, fracture can be modelled by failing particles according to a suitable criterion. When material points are failed, they are assumed to have a null stress tensor. Navas *et al.* (2017)[9] developed a eigensoftening algorithm as an extension for quasi-brittle materials of the eigenerosion proposed by Pandolfi & Ortiz (2012)[10] for fracture of brittle materials. A comparison between both in [9] shows that the eigenerosion algorithm significantly overestimates the tensile stress and the strain peaks, while it captures the forces and crack patterns accurately. On the other hand eigensoftening algorithm agree very well with experimental results in all the aspects. Furthermore, this algorithm has also proof its accuracy for complex fracture patters such the present in fiber reinforces concrete (FRC), [11].

$$G_p^{k+1} = \frac{C_\epsilon}{m_p^{k+1}} \sum_{x_q^{k+1} \in B_\epsilon(x_p^{k+1})} m_q W_q^{k+1} \quad (13)$$

$$m_p^{k+1} = \sum_{x_q^{k+1} \in B_\epsilon(x_p^{k+1})} m_q \quad (14)$$

where $B_\epsilon(x_p^{k+1})$ is the sphere of radius ϵ centered at x_p^{k+1} known as the ϵ -neighborhood of the material point, m_p^{k+1} is the mass of the neighborhood

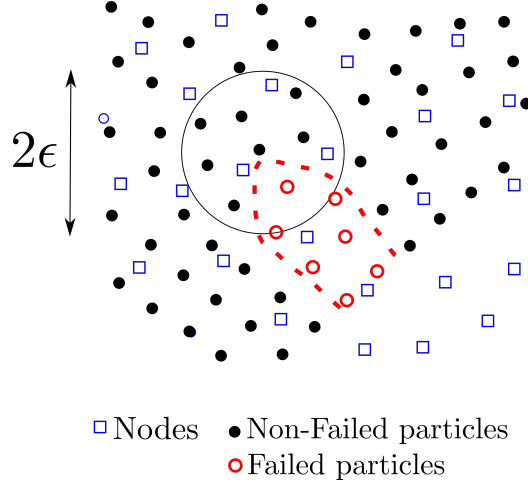


Figure 1: Scheme of a linear cohesive law, where the shaded area is G_f , f_t is the tensile strength, and w_c is the critical opening displacement.

at step $k + 1$, W_q^{k+1} is the current free-energy density per unit mass as the material point x_q^{k+1} of the neighborhood, finally C_ϵ is a normalizing constant. This configuration conveniently is sketched in Figure 1. The material point fails when G_p^{k+1} surpasses a critical energy release rate that measures the material-specific energy, G_F . The convergence of this approach has been analyzed by Schmidt *et al.* (2009)[12], who proof that it converges to the Griffith fracture when discretization size tends to zero. It is necessary to point out that when a material point overpass the critical energy, its contribution to the internal forces vector is set to zero, but its contribution to the mass matrix is maintained. The mass of a material point is discarded only when an eroded material point is not connected to any nodes.

As can be noticed, in the eigenerosion algorithm an energetic criterion is adopted. Due to that fact, unrealistic stress concentration (higher than tensile strength) in quasi-brittle materials, see [9]. To overcome this limitation, the aforementioned authors proposed the concept of eigensoftening to take in to account the gradual failure in quasi-brittle materials. The concept is inspired in the cohesive fracture widely employed in the context of FEM [13]. This gradual failure criterion is plotted in figure , where a linear decreasing cohesive law is presented to illustrate the concept here described. In the picture, the shaded area represents the static fracture energy per unit of area, G_F . As we can see, a cohesive crack appears when the maximum tensile strength, f_t is reached. Once the opening displacement w takes the value of the critical crack displacement w_c , a stress-free crack is attained. For

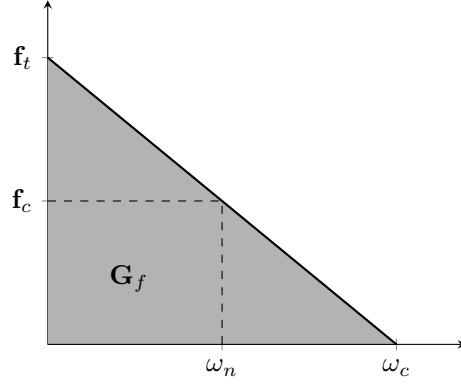


Figure 2: Scheme of a linear cohesive law, where the shaded area is G_f , f_t is the tensile strength, and w_c is the critical opening displacement.

95 intermediate values, w_n , a damage value between zero and one represents the extension to which the material has failed. For the eigensoftening algorithm, a strength criterion for crack initialization was adopted

$$\delta W_{p,\epsilon} = \frac{\partial G_p}{C_\epsilon} = \frac{1}{m_p} \sum_{x_q^{k+1} \in B_\epsilon(x_p^{k+1})} m_q \sigma_{q,I} \delta \epsilon_q \quad (15)$$

$$\delta W_{p,\epsilon} = \frac{\delta \epsilon_p}{m_p} \sum_{x_q^{k+1} \in B_\epsilon(x_p^{k+1})} m_q \sigma_{q,I} \quad (16)$$

$$\delta \sigma_{p,c} = \frac{1}{m_p} \sum_{x_q^{k+1} \in B_\epsilon(x_p^{k+1})} m_q \sigma_{q,I} \quad (17)$$

3. Cases of study and discussion

3.1. Comparison with analytical solution

100 3.2. Brazilian test

3.3. Drop-weight impact test

4. Conclusions

Acknowledgements

The first author acknowledges the fellowship Agustn de Betancourt 262390106114.

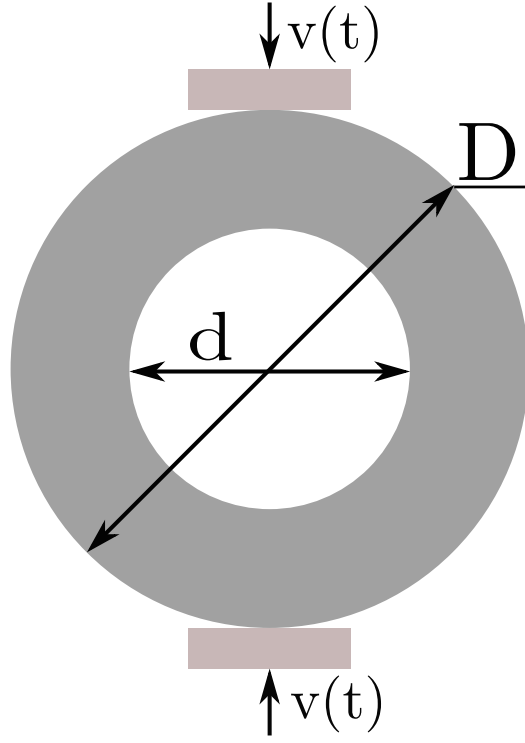


Figure 3: Geometry and boundary condition of the Brazilian test.

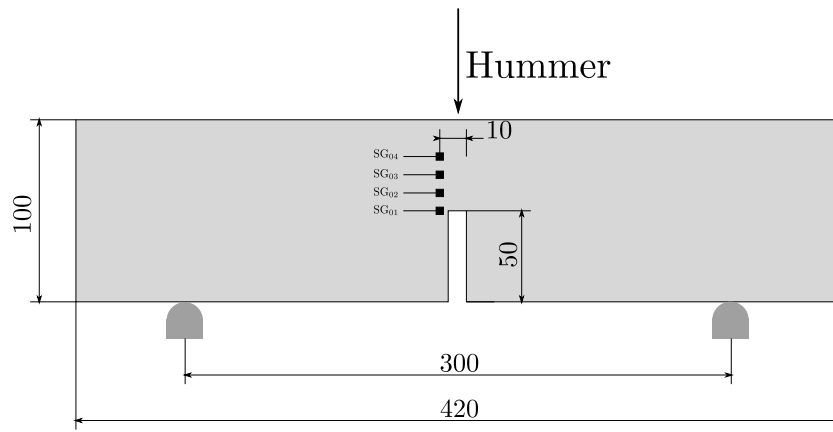


Figure 4: Geometry and boundary condition of the drop-weight impact test.

105 **Appendix A. Explicit Predictor-Corrector algorithm**

Appendix B. Eigensoftening Algorithm

References

- [1] Y. GUO, J. Nairn, Three-dimensional dynamic fracture analysis using the material point method, Computer Modeling in Engineering Sciences 16. 110
- [2] J. Nairn, Material point method calculations with explicit cracks, Computer Modeling in Engineering & Sciences 4 (6) (2003) 649–664. doi:10.3970/cmcs.2003.004.649. URL <http://www.techscience.com/CMES/v4n6/33290>
- 115 [3] H. Tan, J. Nairn, Hierarchical, adaptive, material point method for dynamic energy release rate calculations, Computer Methods in Applied Mechanics and Engineering 191 (2002) 2123–2137. doi:10.1016/S0045-7825(01)00377-2.
- 120 [4] Y. GUO, J. Nairn, Calculation of j-integral and stress intensity factors using the material point method, CMES. Computer Modeling in Engineering Sciences 6.
- 125 [5] D. L. Sulsky, H. Schreyer, Z. Chen, A particle method for history-dependent materials, Computer Methods in Applied Mechanics and Engineering 118 (1) (1994) 179–196. doi:10.1016/0045-7825(94)90112-0.
- [6] M. Arroyo, M. Ortiz, Local maximum-entropy approximation schemes: A seamless bridge between finite elements and meshfree methods, International Journal for Numerical Methods in Engineeringdoi:10.1002/nme.1534.
- 130 [7] E. Jaynes, Information Theory and Statistical Mechanics, The Physical Review 106 (4) (1957) 620–630.
- [8] C. E. Shannon, A Mathematical Theory of Communication, Bell System Technical Journaldoi:10.1002/j.1538-7305.1948.tb01338.x.
- 135 [9] P. Navas, R. Yu, B. Li, G. Ruiz, Modeling the dynamic fracture in concrete: an eigensoftening meshfree approach, International Journal of Impact Engineering 113. doi:10.1016/j.ijimpeng.2017.11.004.

Algorithm Explicit Predictor-Corrector scheme

Update mass matrix:

$$\mathbf{m}_I = N_{Ip}^k m_p,$$

Explicit Newmark Predictor:

$$\vec{v}_I^{pred} = \frac{N_{Ip}^k m_p (\vec{v}_p^k + (1 - \gamma) \Delta t \vec{a}_p^k)}{m_I}$$

Impose essential boundary conditions: At the fixed boundary, set $\vec{v}_I^{pred} = 0$. **Deformation tensor increment calculation.**

$$\begin{aligned} \dot{\varepsilon}_p^{k+1} &= \left[\vec{v}_I^{pred} \otimes \text{grad}(N_{Ip}^{k+1}) \right]^s \\ \Delta \varepsilon_p^{k+1} &= \Delta t \dot{\varepsilon}_p^{k+1} \end{aligned}$$

Update the density field:

$$\rho_p^{k+1} = \frac{\rho_p^k}{1 + \text{tra} [\Delta \varepsilon_p^{k+1}]}.$$

Compute damage parameter: **Balance of forces calculation:** Calculate the total grid nodal force $\vec{f}_I^{k+1} = (1 - \chi) \vec{f}_I^{\text{int},k+1} + \vec{f}_I^{\text{ext},k+1}$ evaluating (??) and (??) in the time step $k + 1$. In the grid node I is fixed in one of the spatial dimensions, set it to zero to make the grid nodal acceleration zero in that direction. **Explicit Newmark Corrector:**

$$\vec{v}_I^{k+1} = \vec{v}_I^{pred} + \gamma \Delta t \frac{\vec{f}_I^{k+1}}{\mathbf{m}_I^{k+1}}$$

Update particles lagrangian quantities:

$$\begin{aligned} \vec{a}_p^{k+1} &= \frac{N_{Ip}^k \vec{f}_I^k}{\mathbf{m}_I^k} \\ \vec{v}_p^{k+1} &= \vec{v}_p^n + \Delta t \frac{N_{Ip}^k \vec{f}_I^k}{\mathbf{m}_I^k} \\ \vec{x}_p^{k+1} &= \vec{x}_p^n + \Delta t N_{Ip}^k \vec{v}_I^k + \frac{1}{2} \Delta t^2 \frac{N_{Ip}^k \vec{f}_I^k}{\mathbf{m}_I^k} \end{aligned}$$

Reset nodal values

Algorithm 2 Compute damage parameter χ_p^{k+1}

Particle status Number of particles: N_p ϵ -neighbourhood of each
 particle p : $B_{\epsilon,p}$ Material data Tensile strength: $f_{t,p}$ Bandwidth
 of the cohesive fracture: $h_{\epsilon,p}$ Critical opening displacement:
 w_c Return damage parameter $\chi := \{\chi_p\}$ $\chi_p \leftarrow \chi_p^k$ p to N_p $\chi_p = 0$
 $\epsilon_{f,p} = 0$ $q \in B_{\epsilon,p}$ $\chi_q < 1$ $\sum m_p \sigma_{p,I} \leftarrow \sum m_p \sigma_{p,I} + m_q \sigma_{q,I}$ $m_p \leftarrow m_p + m_q$
 $\sigma_{p,\epsilon} \leftarrow \frac{1}{m_p} \sum m_p \sigma_{p,I}$ $\sigma_{p,\epsilon} > f_{t,p}$ $\epsilon_{f,p} = \epsilon_{I,p}$ [$\chi_p \neq 1$ $\epsilon_{f,p} > 0$] $\chi_p^{k+1} \leftarrow$
 $\min \left\{ 1, \max \left\{ \chi_p^k, \frac{(\epsilon_{I,p} - \epsilon_{f,p}) h_{\epsilon,p}}{w_c} \right\} \right\}$

- [10] A. Pandolfi, M. Ortiz, An eigenerosion approach to brittle fracture., International Journal for Numerical Methods in Engineering 92 (2012) 694–714.
- 140 [11] P. Navas, R. Yu, G. Ruiz, Meshfree modeling of the dynamic mixed-mode fracture in frc through an eigensoftening approach, Engineering Structures 172. doi:10.1016/j.engstruct.2018.06.010.
- [12] B. Schmidt, F. Fraternali, M. Ortiz, Eigenfracture: an eigendeformation approach to variational fracture., SIAM J. Multiscale Model. Simul. 7 (2009) 1237–1266.
- 145 [13] M. Ortiz, A. Pandolfi, Finite-deformation irreversible cohesive elements for three-dimensional crack-propagation analysis., International Journal for Numerical Methods in Engineering. 44 (1999) 1267–1282.